

Kozumplik, Joanne (ASRC)

469483

**From:** STIC-ILL  
**Sent:** Friday, October 24, 2003 9:40 AM  
**To:** Kozumplik, Joanne (ASRC)  
**Subject:** FW: 10038600

-----Original Message-----

**From:** Mellerson, Kendra  
**Sent:** Friday, October 24, 2003 9:37 AM  
**To:** STIC-ILL  
**Subject:** FW: 10038600

-----Original Message-----

**From:** Gakh, Yelena  
**Sent:** Thursday, October 23, 2003 6:23 PM  
**To:** STIC-EIC1700  
**Subject:** 10038600

Dear Kendra,

please order the following:

1. TITLE High-throughput characterization of composition-spread manganese oxide films with a scanning SQUID microscope

AUTHOR(S): Hasegawa, T.; Kageyama, T.; Fukumura, T.; Okazaki, N.; Kawasaki, M.; Koinuma, H.; Yoo, Y. K.; Duewer, F.;

Xiang, X.-D.

CORPORATE SOURCE: Materials and Structures Laboratory, Tokyo Institute of Technology, Midori-ku, Yokohama, 226-8503, Japan

SOURCE: Applied Surface Science (2002), 189(3-4), 210-215

Thanks,

Yelena

-----  
Yelena G. Gakh, Ph.D.

Patent Examiner  
USPTO, cp3/7B-08  
(703)306-5906



ELSEVIER

NOTICE: This material may be protected  
by copyright law (Title 17, U.S. Code)

applied  
surface science

Applied Surface Science 189 (2002) 210–215

www.elsevier.com/locate/apsusc

## High-throughput characterization of composition-spread manganese oxide films with a scanning SQUID microscope

T. Hasegawa<sup>a,b,\*</sup>, T. Kageyama<sup>a</sup>, T. Fukumura<sup>c</sup>, N. Okazaki<sup>b</sup>, M. Kawasaki<sup>b,c</sup>,  
H. Koinuma<sup>a,b</sup>, Y.K. Yoo<sup>d</sup>, F. Duewer<sup>d</sup>, X.-D. Xiang<sup>d</sup>

<sup>a</sup>Materials and Structures Laboratory, Tokyo Institute of Technology, Midori-ku, Yokohama 226-8503, Japan

<sup>b</sup>Combinatorial Materials Exploration and Technology (COMET), Midori-ku, Yokohama 226-8503, Japan

<sup>c</sup>Department of Innovative and Engineered Materials, Tokyo Institute of Technology, Midori-ku, Yokohama 226-8502, Japan

<sup>d</sup>Environmental Energy Technologies Division, Lawrence Berkeley National Laboratory, Berkeley, CA 94720, USA

Accepted 30 October 2001

### Abstract

We have performed high-throughput characterization of composition-spread  $\text{La}_{1-x}\text{Ca}_x\text{MnO}_3$  (LCMO) and  $\text{Nd}_{1-x}\text{Sr}_x\text{MnO}_3$  (NSMO) films, fabricated by the precursor technique, with a scanning SQUID microscope (SSM). In both films, SSM successfully observed spatial variation of magnetic field, corresponding to magnetic phase transitions with respect to chemical composition. The obtained magnetic phase diagrams basically reproduced those reported in bulk materials. However, several distinctive differences have also been noted. For instance, the region identified as a charge ordered insulator in LCMO revealed intense field, suggesting the occurrence of phase separation into ferromagnetic and non-magnetic states. These results confirm that SSM possesses sufficient analytical performance for high-throughput characterization of combinatorial magnetic libraries in composition spread form. © 2002 Elsevier Science B.V. All rights reserved.

PACS: 07.79.-v; 68.37.-d; 75.60.Ch; 75.70.Ak

Keywords: Manganese oxide; Thin film; Combinatorial technique; Scanning SQUID microscope; Magnetic phase diagram

### 1. Introduction

It is well known that perovskite-type manganese oxides show a wide variety of electronic and magnetic properties such as colossal magneto-resistance and charge ordering as functions of temperature and chemical composition [1]. Therefore, it is of crucial importance to systematically investigate the doping

effects in these systems both for understanding the underlying physics and for exploring their practical applications. Indeed, great efforts have been devoted to the phase diagram studies [1]. However, these works usually require large numbers of high quality single crystals and careful characterization of individual samples and thus they are very time-consuming.

Recent progress in combinatorial techniques starts changing the material research works completely [2]. They not only accelerate the searches for new materials but also considerably systematize them, because experimental errors associated with sample preparations and analyses can be minimized.

\*Corresponding author. Present address: Materials and Structures Laboratory, Tokyo Institute of Technology, Midori-ku, Yokohama 226-8503, Japan. Tel./fax: +81-45-924-5363.  
E-mail address: t.hasegawa@rlem.titech.ac.jp (T. Hasegawa).

To characterize combinatorial manganite samples, on the other hand, new microscopic tools accessible to local magnetic properties of small pixels are highly desired. For such a purpose, scanning probe microscopes (SPMs) are most suitable, and several magnetic probes have been developed so far [3–7]. These include magnetic force microscope (MFM) [3,4], scanning Hall probe microscope (SHPM) [5] and scanning SQUID microscope (SSM) [6,7]. MFM is now widely used to image magnetic structures in a sub-micron scale. However, it is hardly applicable to combinatorial materials, because its magnetic signal originating from magnetostatic interaction between probe and sample does not directly reflect the magnitude of local magnetic moment. In contrast, SSM is a quantitative probe with extremely high field sensitivity, so that it is capable of sensing even weak field of thin film samples, although its spatial resolution is limited by the SQUID ring size, several micrometers [6,7].

Here, we report the combinatorial characterization of manganese oxide films,  $\text{La}_{1-x}\text{Ca}_x\text{MnO}_3$  (LCMO) and  $\text{Nd}_{1-x}\text{Sr}_x\text{MnO}_3$  films (NSMO), in composition-spread form with a SSM. The microscope has successively detected local magnetic field, generated from domain boundaries, across the films, yielding magnitude of magnetic moment as a function of chemical composition,  $x$ . The obtained results are basically consistent with the magnetic phase diagrams reported in bulk materials. However, distinctive disagreements have also been found.

## 2. Experimental

Composition-spread films of LCMO and NSMO were fabricated by the so-called precursor method. The detailed film growth procedures were described elsewhere [8]. Here, it should be noted that the present composition-spread films experienced sintering at a high temperature, 1000 °C. Accordingly, they are relatively free from lattice distortion arising from the lattice mismatch between film and substrate,  $\text{LaAlO}_3$ . But there still remains a small substrate effect, as reported by Yoo et al. [8].

An SSM, equipped with a miniature SQUID ring (10  $\mu\text{m}$  OD) near an edge of an AFM cantilever, was used to sense local magnetic field perpendicular to the film surface  $B_z$  without external field [7]. The sample

set on variable-temperature sample stage was mechanically scanned against the SQUID sensor (scanning range  $>10\text{ mm} \times 10\text{ mm}$ ), keeping the tip-sample distance constant,  $\sim 5\text{ }\mu\text{m}$ . Measurement temperature was controlled between 3 and  $\sim 100\text{ K}$ , using a heater surrounding the sample stage. The field sensitivity and spatial resolution are 50 pT (dc level) and 5  $\mu\text{m}$ , respectively [7].

## 3. Results and discussion

Fig. 1 shows two-dimensional magnetic images ( $300\text{ }\mu\text{m} \times 300\text{ }\mu\text{m}$ ) observed by SSM at several locations on the composition-spread LCMO film. Along the horizontal axis, Ca composition  $x$  varies. One can clearly see magnetic structures of several tens of microns, representing magnetic domains. A ferromagnet, in general, is not homogeneously polarized, but is divided into domains with different magnetic axes. In thin films, the magnetic moments tend to lie parallel to the film surface in order to reduce the magnetostatic energy. If this is the case, domain boundaries emit or absorb magnetic field, which is detected as positive or negative  $B_z$  by SSM, as shown in Fig. 1. Namely, white and black regions indicate domain boundaries, while the regions inside the domains are colored gray.

Fig. 2(b) is a one-dimensional  $B_z$  profile along the horizontal direction in Fig. 1. An oscillating structure is evidently visible, reflecting again the magnetic domains. When magnetic domains with in-plane magnetization are periodically arranged along a lateral direction, as illustrated in Fig. 3(a), the  $z$ -component of magnetic field generated from a boundary  $b_z$  is given by [9]:

$$b_z(x, z) = \frac{M_s}{2\pi} \sum_{n=-\infty}^{n=+\infty} (-1)^n \ln \frac{z^2 + (x + nd)^2}{(z + t)^2 + (x + nd)^2} \quad (1)$$

where  $M_s$  is the spontaneous magnetization,  $d$  the domain width,  $t$  the thickness of the film,  $x$  and  $z$  are horizontal and vertical positions defined in Fig. 3(a). Since SSM counts numbers of magnetic flux penetrating a SQUID ring, the  $B_z$  value observed by SSM is finally expressed as an integral,

$$B_z(x, h) = \left( \frac{1}{S_{\text{ring}}} \right) \int_{\text{ring}} b_z(x, h) dS \quad (2)$$

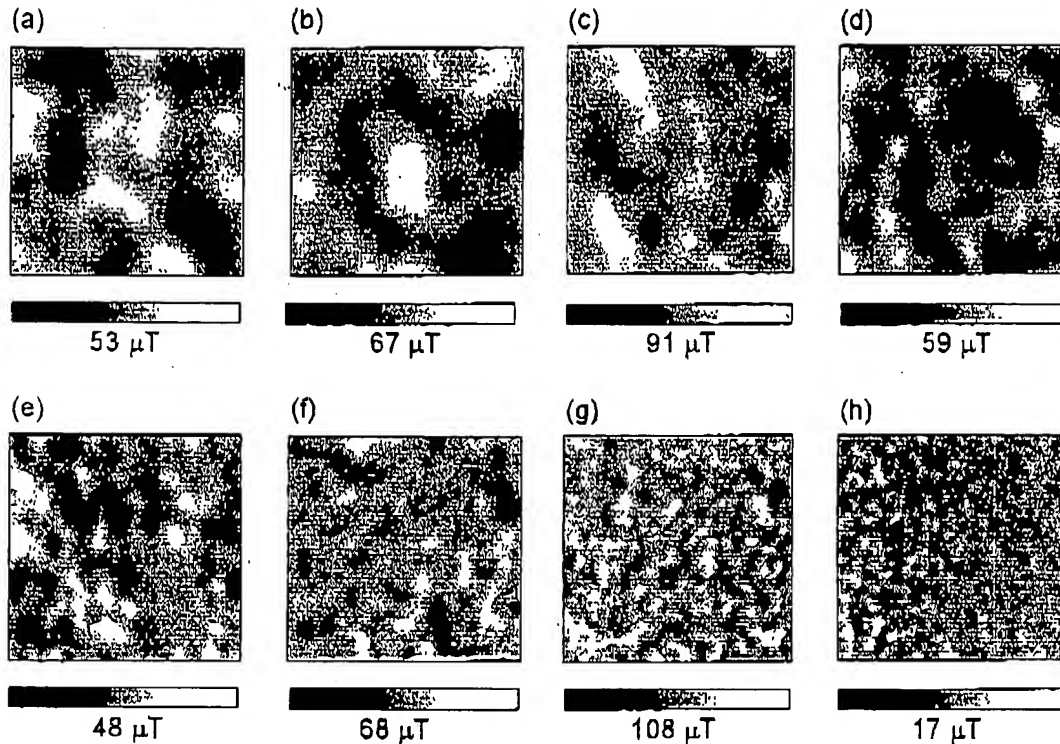


Fig. 1. Two-dimensional magnetic images of composition-spread LaCaMnO film observed by SSM at 3 K. The scanning areas are  $300 \times 300 \mu\text{m}^2$  for all images. (a)  $x = 0.078\text{--}0.099$ ; (b)  $x = 0.099\text{--}0.119$ ; (c)  $x = 0.182\text{--}0.202$ ; (d)  $x = 0.330\text{--}0.351$ ; (e)  $x = 0.449\text{--}0.470$ ; (f)  $x = 0.504\text{--}0.524$ ; (g)  $x = 0.643\text{--}0.664$ ; (h)  $x = 0.868\text{--}0.888$ .

where  $h$  is the probe-sample distance, and  $S_{\text{ring}}$  the area of SQUID ring. Fig. 3(b) exhibits  $B_z$  profiles calculated for various  $t$  values. The maximum field,  $B_z^{\text{max}} \equiv B_z(0, h)$ , is plotted against  $t$ , in Fig. 3(c). If one observes both  $d$  and  $B_z^{\text{max}}$  experimentally,  $M_s$  can be evaluated using Eq. (2).

Fig. 2(c) is the envelope of  $B_z$  corresponding to  $B_z^{\text{max}}$  as a function of  $x$ . The  $d$  values, deduced by the fast Fourier transformation (FFT) analysis of  $B_z$  profile, are plotted in Fig. 2(d). Fig. 2(e) is an  $M_s$  curve computed from Fig. 2(c) and (d). In the present case,  $d$  is weakly dependent on  $x$ . Thus, the  $B_z^{\text{max}}$  profile is almost proportional to  $M_s$ .

From Fig. 2(e), it is evident that the magnitude of  $M_s$  dramatically changes with  $x$ .  $M_s$  shows a local minimum at  $x = 0.2$ , which is equivalent to the phase boundary between ferromagnetic insulator (FI) and ferromagnetic metal (FM) states. After it is maximized around  $x = 0.3$ ,  $M_s$  is abruptly suppressed at  $x = 0.5$ , where charge ordering takes place. Thus, the observed  $B_z$  profile in the range  $x = 0\text{--}0.5$  is quite consistent with the magnetic properties of bulk materials in

Fig. 2(a) [10]. In contrast, the present SSM results remarkably differ from those of bulk studies for  $x > 0.5$ . According to the bulk phase diagram, the charge order insulator (COI) phase is located at  $x > 0.5$ , where no spontaneous magnetization is expected. However, we have found intense field in the region, which is comparable to that of FM. This strongly suggests that phase separation into ferromagnetic and charge order non-magnetic phases occurs.

Around  $x = 0.9$ ,  $M_s$  is rapidly reduced, indicating that AF order sufficiently develops there. Even for  $x > 0.9$ , however, we have detected finite  $B_z$  of  $1 \mu\text{T}$  level. Indeed, the SSM image near the COI/AF phase boundary in Fig. 1(h) clearly resolves magnetic domains in the higher  $x$  side. This implies that the AF moments are slightly canted, resulting in appearance of gross magnetization perpendicular to the AF spins. The present observation is a very good demonstration for high field sensitivity of the SQUID microscope.

Fig. 4 summarized the results of combinatorial characterization of NCMO film at various temperatures.

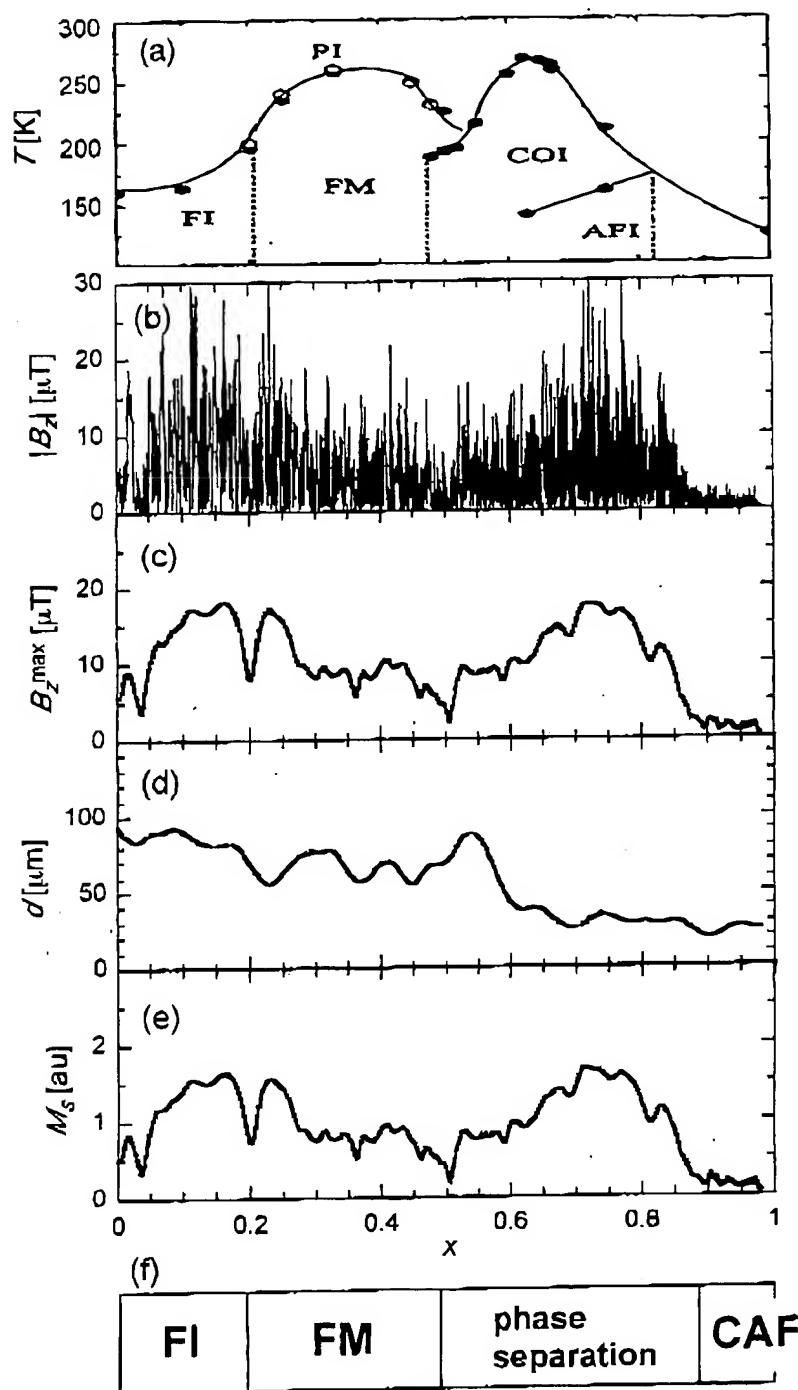


Fig. 2. Local magnetic properties of composition-spread LaCaMnO film at 3 K: (a) bulk phase diagram [9]; (b) one-dimensional  $B_z$  profile across the film; (c) envelope of  $B_z$  profile; (d) domain width  $d$  estimated from the oscillation period of  $B_z$ ; (e) calculated spontaneous magnetization  $M_s$ ; (f) proposed magnetic phase diagram.

Large  $B_z$  values, reaching to 50  $\mu\text{T}$ , was observed in the region  $x < 0.55$ , which corresponds to the FM phase [11].  $B_z$  is diminished to zero around  $x = 0.6$ , where the COI phase appears. Meanwhile, we found

finite  $B_z$  for  $x = 0.7\text{--}0.9$  with a local maximum at 0.8, representing the canted AF (CAF) state. From Fig. 4, it can be concluded that the magnetic properties of NCMO system are essentially independent of

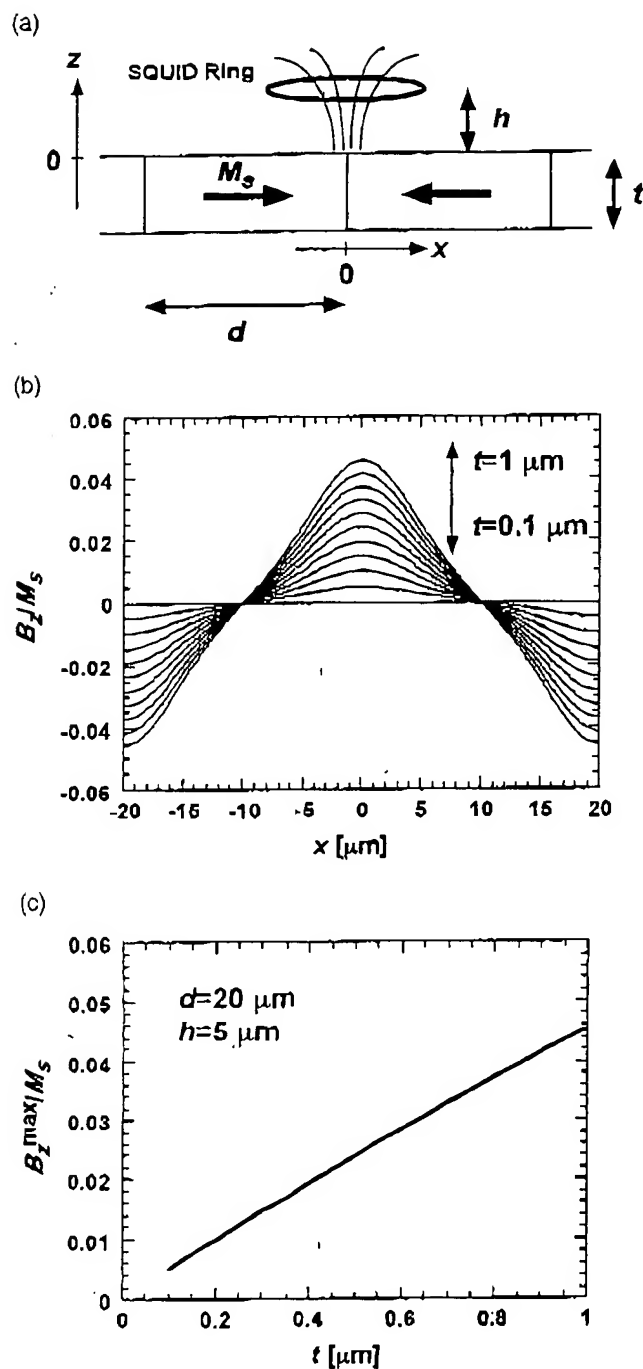


Fig. 3. (a) Calculated magnetic field generated from magnetic domains with in-plane magnetization; (b)  $B_z$  profiles across domains for various film thickness  $t$ ; (c) maximum field  $B_z^{\text{max}}$  as a function of  $t$ .

temperature below 100 K. A new finding is that the CAF survives up to 100 K in contrast to the bulk phase diagram indicating the disappearance of CAF phase around 70–80 K.

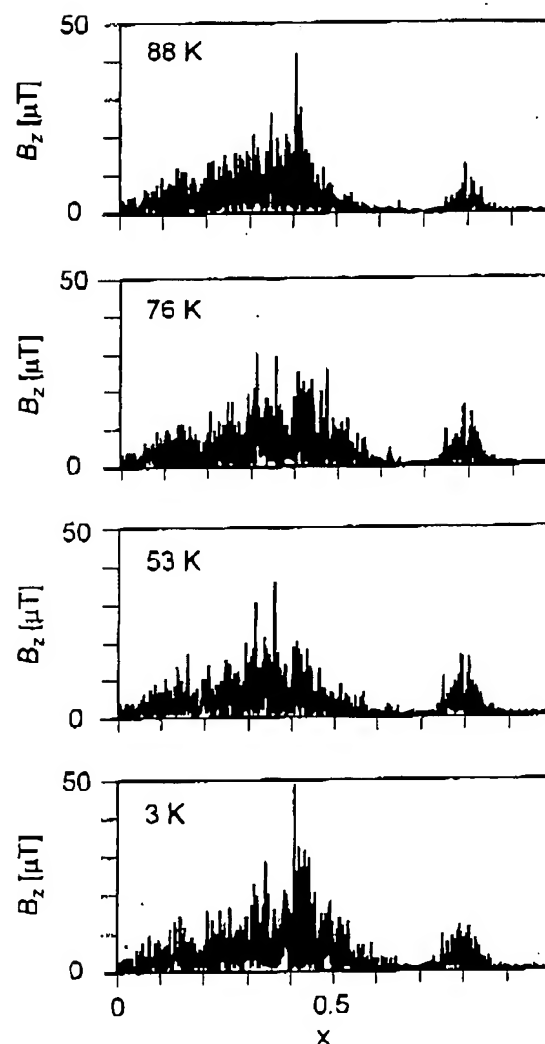
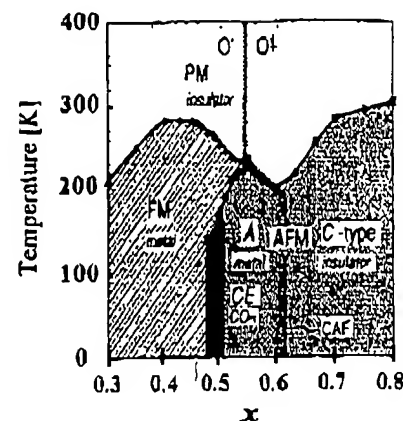


Fig. 4. Local magnetic properties of composition-spread NdSrMnO film at various temperatures. The top panel is the bulk phase diagram reported by Kajimoto et al. [11].

#### 4. Summary

We have demonstrated that local magnetic properties of manganite films in composition-spread form can be rapidly characterized by the SSM. From the observed domain sizes and magnitude of magnetic field, arising from domain boundaries, spontaneous magnetization  $M_s$  was quantitatively calculated as a function of alkaline earth composition  $x$ . The resulting  $M_s$  distributions are consistent with the bulk phase diagrams, although a few remarkable disagreements such as magnetic behavior of COI phase of LCMO were recognized. The present observations confirm that SSM is quite useful for analyzing combinatorial magnetic libraries composed of micrometer order pixels.

#### References

- [1] M. Imada, A. Fujimori, Y. Tokura, *Rev. Mod. Phys.* 70 (1998) 1039.
- [2] X.-D. Xiang, X. Sun, G. Brinco, Y. Lou, K.-A. Wang, H. Chang, W.G. Wallace-Freedman, S.-W. Chen, P.G. Schlutz, *Science* 23 (1995) 1738.
- [3] Y. Martin, H.K. Wickramasinghe, *Appl. Phys. Lett.* 50 (1987) 1455.
- [4] Y. Martin, D. Ruger, H.K. Wickramasinghe, *Appl. Phys. Lett.* 52 (1988) 24.
- [5] A.M. Chang, H.D. Hallen, L. Harriott, H.F. Hess, H.L. Kao, J. Kwo, R.E. Miller, R. Wolfe, J. van der Ziel, T.Y. Chang, *Appl. Phys. Lett.* 61 (1992) 1974.
- [6] J.R. Kirtley, M.B. Ketchen, K.G. Stawiasz, J.Z. Sun, W.J. Gallagher, S.H. Blanton, S.J. Wind, *Appl. Phys. Lett.* 66 (1995) 1336.
- [7] T. Morooka, S. Nakayama, A. Odawara, M. Ikeda, S. Tanaka, K. Chinone, *IEEE Trans. Appl. Supercond.* 5 (1999) 3491.
- [8] Y.-K. Yoo, F. Ducwer, H. Yang, D. Yi, J.-W. Li, X.-D. Xiang, *Nature* 406 (2000) 704.
- [9] D. Craik, *Magnetism*, Wiley, New York, 1995.
- [10] P. Schiffer, A.P. Ramirez, W. Bao, S.-W. Cheong, *Phys. Rev. Lett.* 75 (1995) 3336.
- [11] R. Kajimoto, H. Yoshizawa, H. Kawano, H. Kuwahara, Y. Tokura, K. Ohoyama, M. Ohashi, *Phys. Rev. B* 60 (1999) 9506.